Phys Chem Minerals (2003) 30: 177–183
DOI 10.1007/s00269-003-0298-2

ORIGINAL PAPER

A. Cattaneo · A. F. Gualtieri · G. Artioli

Kinetic study of the dehydroxylation of chrysotile asbestos with temperature by in situ XRPD

Received: 10 April 2002 / Accepted: 7 January 2003

Abstract The kinetics of the dehydroxylation of chrysotile was followed in situ at high temperature using real-time conventional and synchrotron powder diffraction (XRPD). This is the first time kinetics parameters have been calculated for the dehydroxylation of chrysotile. The value of the order of the reaction mechanism calculated using the Avrami model indicates that the rate-limiting step of the reaction is a one-dimensional diffusion with an instantaneous nucleation or a decelerated rate of nucleation of the reaction product. Hence, the rate-limiting step is the one-dimensional diffusion of the water molecules formed in the interlayer region by direct condensation of two hydrogen atoms and an oxygen atom. The calculated apparent activation energy of the reaction in the temperature range 620–750 °C is 184 kJ mol^{-1}. The diffusion path is along the axis of the fibrils forming the fibers. The amorphous or short-range ordered dehydroxylate of chrysotile is extremely unstable because forsterite readily nucleates in the Mg-rich regions. Moreover, it is less stable than the dehydroxylate of kaolinite, the so-called metakaolinite, which forms mullite at about 950 °C. This difference is interpreted in terms of the different nature of the two ions Mg^{2+} and Al^{3+} and their function as glass modifier and glass-forming ion, respectively.

Keywords Asbestos · Chrysotile · In situ powder diffraction · Reaction kinetics · Activation energy

A. Cattaneo
Dipartimento di Medicina del Lavoro,
Università di Milano, 20122 Milano, Italy

A. F. Gualtieri (✉)
Dipartimento di Scienze della Terra,
Università di Modena e Reggio Emilia, 41100 Modena, Italy
Fax: 0039-059-2055887
e-mail: alex@unimo.it

G. Artioli
Dipartimento di Scienze della Terra,
Università di Milano 20133 Milano, Italy

Introduction

Chrysotile belongs to the serpentine group and has an ideal chemical formula, $Mg_3Si_2O_5(OH)_4$. Serpentine species are 1:1 sheet silicates characterized by the stacking of a tetrahedral layer (T) and an octahedral layer (O). The T layer is formed by the two-dimensional polymerization of silicon-centered tetrahedra sharing three out of four apical oxygen atoms with the other tetrahedra. Unshared oxygen atoms are bonded to Mg atoms of the octahedral sheet. Polymorphism in serpentine originates from the different curvature of the TO layers, caused by the misfit between the tetrahedral sheet, ideally 9.43 Å long, and the octahedral sheet, ideally 9.41Å (Wicks and O'Hanley 1988).

Given its outstanding technological properties, asbestos has been utilized since ancient times for a large number of applications. Unfortunately, the peculiar fibrous morphology responsible for its properties is also the cause of hazard (Guthrie 1992; Fubini and Otero Areán 1999). Because asbestos is now considered a carcinogenic material, its elimination from the environment has become a priority in many industrialized countries. It is now well established that asbestos-containing materials can be thermally transformed and recycled. In fact, when fired at temperatures higher than 1000 °C, either serpentine or amphibole species transform into Mg–Fe silicates, which may be recycled at no cost in traditional ceramics (Gualtieri and Tartaglia 2000). Thus, the understanding of the mechanism controlling the thermal decomposition of chrysotile at high temperature has practical implications for the design of the treatment plants and control of the firing processes of asbestos-containing materials.

Literature data show that chrysotile becomes amorphous during dehydroxylation through a process in which the hydroxyl ions, occupying 75% of the octahedral Mg sites, are eliminated from the crystal structure. The resulting phase contains some elements of the original structure necessary for the *topotactic* (?) nucleation of new crystalline phases (Martin 1977). Bowen and Tuttle (1949)

obtained forsterite and talc after heating chrysotile in water vapor atmosphere. Nelson and Roy (1954) and Brindley and Zussman (1957) observed the development of a broad reflection at low angles ($d = 14$–15 Å) that disappeared before the nucleation of forsterite. Ball et al. (1963) suggested that during the dehydroxylation of serpentine, protons migrate to a reaction zone where water molecules are condensed and liberated. Mg and Si ions countermigrate, keeping the Mg–Si ratio 3:2 to retain electrical neutrality, whereas the oxygen framework later hosts all the Mg and Si ions. This process leads to the segregation of Mg-rich and Si-rich regions and to the formation of an amorphous dehydroxylate. Later, forsterite crystallization takes place from ordering of cations in the Mg-rich regions. The development of enstatite is related to the Si-rich regions. Brindley and Hayami (1965) confirmed the first stage of the reaction sequence described by Ball and Taylor (1963), but claimed that some degree of order must persist in the anhydrous precursor of forsterite. They also supported the fact that all the Mg in serpentine is necessary for the formation of forsterite-segregating residual silica. Thus, the appearance of enstatite at higher temperatures is due to the reaction of this phase with forsterite. In some samples the dehydroxylation seems to be a multistep process (Datta et al. 1986) due to the presence of two types of chrysotile particles with different reactivity. The NMR data of Mackenzie and Meinhold (1994) showed the appearance of a broad peak apparently associated with the first of the two weight-loss processes and probably due to the presence of an amorphous anhydrous phase called dehydroxylate I. Above 700 °C the resonance of chrysotile decreases and a sharp new resonance associated with forsterite appears. An extra peak survives up to 800 °C. It is typical of the 1:1 structures and was related to an amorphous phase retaining some structural elements of chrysotile. This Si-rich phase is called dehydroxylate II. Above 800 °C a broad peak corresponding to amorphous silica appears. Forsterite nucleates within the dehydroxylate I whereas amorphous silica forms at the expense of the dehydroxylate II. Enstatite grows at 1130–1150 °C by the reaction of excess silica and forsterite.

In this work, the kinetics of chrysotile dehydroxylation is followed in situ at high temperature using real-time conventional and synchrotron powder diffraction (XRPD). The kinetic analysis using the classical Avrami models yields parameters useful for the interpretation of the reaction mechanism and allows the calculation of the reaction apparent activation energies. To our knowledge, this is the first time kinetics parameters have been calculated for the reaction of dehydroxylation of chrysotile.

Experimental

The sample investigated here is a natural alpine chrysotile from Balangero (Torino, Italy) whose main phase is clinochrysotile $2Mc_1$. Albeit impure, this specific sample was selected because it is representative of the asbestos raw materials used in the past 50 years for a variety of industrial applications.

The quantitative phase analysis (QPA) of the sample was performed using the Rietveld method (Rietveld 1969; Bish and Howard 1988; Hill 1991). Prior to the XRPD analysis, the sample was hand-ground for about 10 min in an agate mortar to achieve a suitable particle size for powder-diffraction experiments. To minimize asbestos amorphization, which occurs by overgrinding asbestos (Suquet 1989), acetone was used as dispersing liquid because it reduces grinding times and consequently the risks of amorphization (Papirer and Roland 1981). The powder sample was side-loaded on an Al holder, and data collection was performed using a CuKα monochromatized radiation in a conventional Bragg–Brentano (BB) parafocusing geometry. Data were collected in the angular range 8–100 °2ϑ with steps of 0.02 °ϑ and 10 s step^{-1}, divergence slit of 1°, and receiving slit of 0.2 mm. The dataset was refined using GSAS (Larson and Von Dreele 1994).

Thermal analyses (TG, DTA) were carried out in air using a Seiko TG/DTA 6300 instrument and a heating rate of 10 °C min^{-1} up to 1200 °C.

The temperature-induced reaction kinetics of the chrysotile sample were studied using both conventional and synchrotron real-time powder diffraction.

In situ experiments with a conventional X-ray source were in part accomplished using a Philips PW 1710 diffractometer in parafocusing Bragg–Brentano geometry at the Department of Physical Chemistry of the University of Pavia (Italy). The experimental setup is characterized by a divergent 0.5° slit on the primary graphite-monochromatized beam, a receiving 0.1-mm slit, and a heating chamber (Anselmi–Tamburini et al. 1983). The sample holder is composed of a metal block surrounded by a U-shaped furnace, and the heating element is a platinum spiral resistance. Data were collected in air with a step size of 0.02 °2θ and 1 s step^{-1}. The time-resolved isothermal runs for the kinetic analysis were performed in the angular ranges 10–15 and 22–27 °2θ in order to follow the decrease of the integrated intensities of the (002) and (004) chrysotile reflections. The evolution of the same peaks was followed in isothermal conditions at 690, 710, 735, and 750 °C. The heating rate was 75 °C min^{-1}. The total experimental time varied from 2 h at 750 °C to 20 h at 690 °C.

Another dataset was collected at the Dipartimento di Scienze della Terra, University of Milan (Italy) using a Philips X'Pert PW 3701 powder diffractometer in parafocusing Bragg–Brentano vertical θ–θ geometry. The experimental configuration was characterized by a divergent 0.5° slit on the incident graphite-monochromatized beam, a receiving 0.1 mm slit on the diffracted beam. The diffractometer is equipped with a PMP 1600 hot chamber (Dapiaggi et al. 2002). Temperature stability is assured by two alumina fiber blocks heated by two $MoSi_2$ resistances. The sample can be rotated, for a better temperature homogeneity and higher counting statistics. The chamber is composed of a dense alumina disk and the sample holder is placed over a cold finger. The motorized sample height positioner keeps the sample surface at the goniometer axis level, compensating for all thermal expansion effects of both the spinner and the sample. Isothermal data were collected in air, with an angular step size of 0.04 °2θ and 0.5 s step^{-1}. The time-resolved isothermal runs for the kinetic analysis were performed in the ranges 9.5–15 and 21–27 °2θ to follow the decrease of the (002) and (004) reflections of chrysotile. The evolution of the same peaks was followed under isothermal conditions collecting data at 635, 655, 675, and 695 °C. The heating gradient to reach the isothermal temperature was 30 °C min^{-1} and the total experimental time varied from 1.2 h at 695 °C to 16 h at 635 °C. The determination of the variation of the integrated peak intensities in temperature was possible using the graphics routines in GSAS (Larson and Von Dreele 1994).

A third dataset was collected using synchrotron diffraction at the Italian beamline BM8 GILDA at ESRF (Grenoble, France) with a Debye–Scherrer setup suitable for kinetic studies (Meneghini et al. 2001). The wavelength calibrated using standard LaB_6 was 0.61993 Å. The collimated synchrotron beam irradiates the powder sample in a rotating 0.7-mm capillary. In situ conditions

were reached nearly instantaneously using a heating-gun system placed below the capillary (Norby 1997). The temperature calibration was obtained using the thermal expansion of Si (Swenson 1983). The detector is a translating image plate system (TIPS) described by Norby (1997). The translating movement is imposed on the basis of the dynamic experimental time. The time-resolved data were collected in nonisothermal mode (with a heating rate equal to that of the thermal analysis, i.e., 10 °C min^{-1}) and in isothermal mode at 620, 630, and 640 °C. The isothermal conditions were readily reached in about 5 min. The total experimental time varied from 0.3 h at 640 °C to about 2 h at 620 °C. The procedure for the data reduction and extraction of the integrated intensities of the (00*l*) chrysotile reflections are well described in Gualtieri et al. (1997). As an example, Fig. 1 is a three dimensional (intensity-2θ-temperature) plot showing the temperature-dependent reaction of dehydroxylation of chrysotile followed by monitoring the decrease of the integrated area of the (002) peak in the temperature range 600–800 °C. Again, the determination of the variation of the integrated peak intensities in temperature was possible using the graphics routines in GSAS (Larson and Von Dreele 1994).

Results

Sample characterization and TA analyses

The results of the QPA of the asbestos sample showed a mixture of chrysotile (66 wt%), magnetite (17 wt%), calcite (13 wt%), brucite (3 wt%), and diopside (< 1 wt%).

The results of the TA analysis are reported in Fig. 2. The DTA pattern shows a broad endothermic peak in the temperature range 600–800 °C related to the dehydroxylation of chrysotile. The associated weight loss is 12.0 wt%. A sharp exothermic peak is shown at ca. 800 °C. The DTG curve shows a peak at ca. 400 °C related to the decomposition of brucite and a split peak due to the dehydroxylation reaction of chrysotile and calcite decomposition at about 750 °C.

Nonisothermal XRPD phase analysis

The main original phases in the investigated sample are clino-chrysotile, magnetite, and calcite. Figure 3 depicts the evolution of the integrated intensities of the original and the newlyformed phases in the investigated system during the nonisothermal run. The following peaks were followed: the (002) and the (004) reflections of chrysotile; the (130) and the (122) of forsterite; the (104) of calcite; and the (311) of magnetite (spinel). Below 750 °C, the qualitative phase analysis showed the coexistence of crystals of calcite, magnetite, the spinel phase (JCPDS card 25–0417), and forsterite (JCPDS card 31–0795). The integrated intensities of chrysotile decreased starting

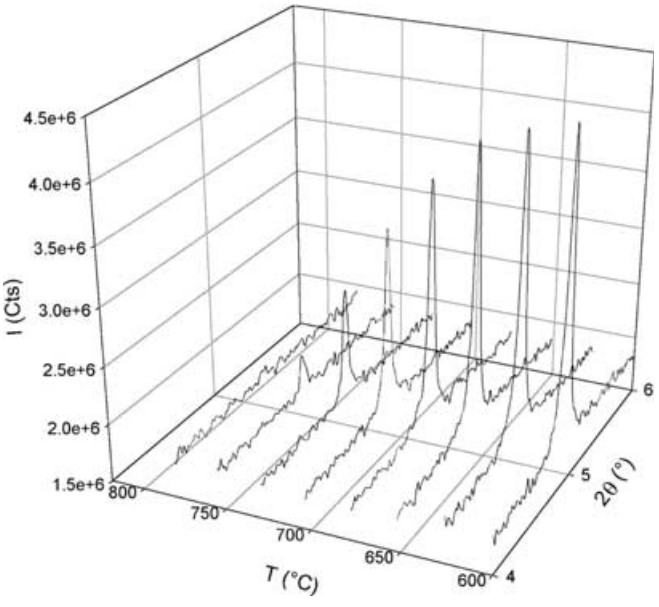

Fig. 1 Selected 2θ range of the three-dimensional real-time synchrotron powder diffraction sequence to follow the evolution of the (002) chrysotile peak in the temperature range 600–800 °C

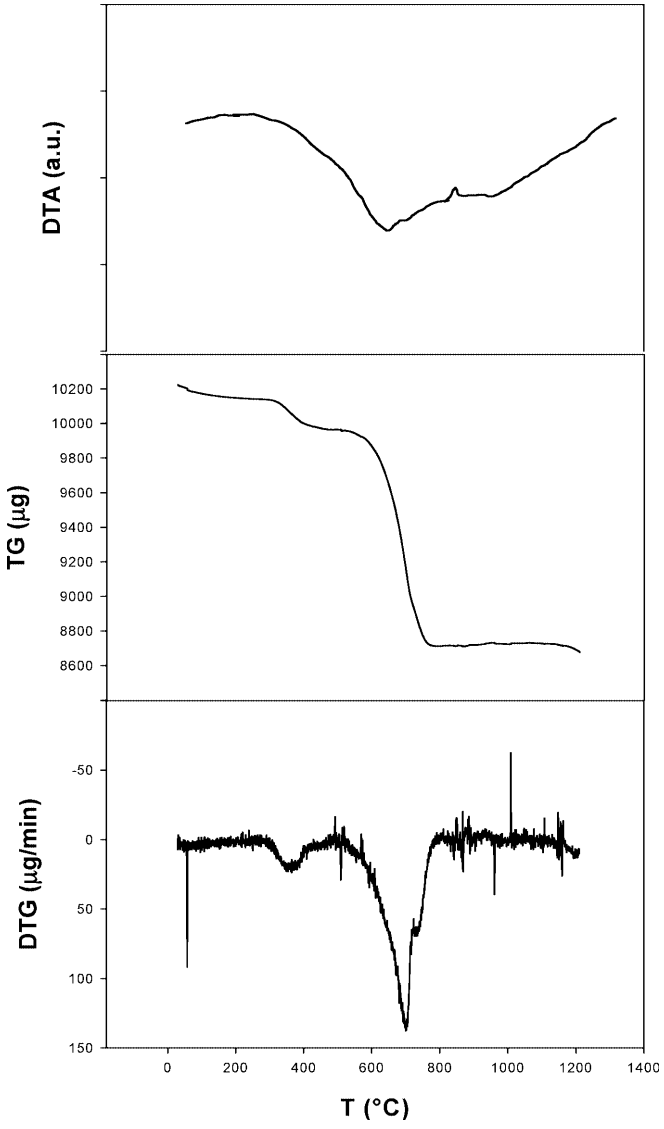

Fig. 2 Thermal analysis (*DTA, TG, DTG*) of the investigated chrysotile sample using a heating rate of 10 °C min^{-1}

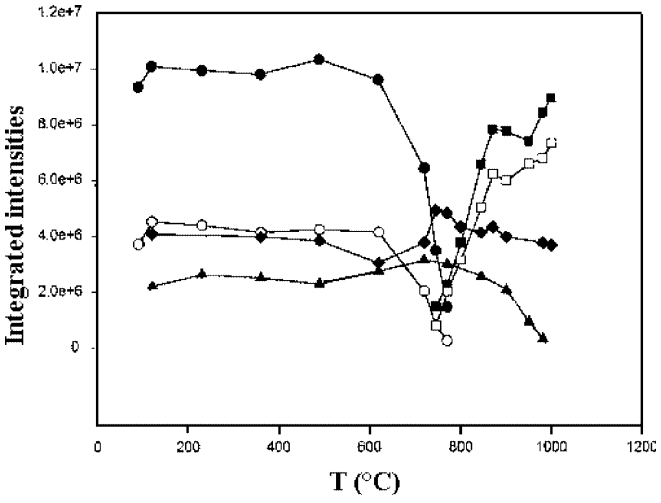

Fig. 3 Temperature variation of the integrated intensities of the main diffraction peaks relative to the phases observed during the transformation of the natural chrysotile sample. *Circles* Chrysotile; *squares* forsterite; *black triangle* calcite; *black diamonds* spinel

from 600 °C. At 800 °C, the chrysotile peaks were no longer observed. Calcite started to decompose above 750 °C with the (104) Bragg reflection, which slowly decreased and disappeared at about 900 °C. The crystallization of forsterite began before chrysotile was totally decomposed. The results show that the two major impurities do not influence the reaction kinetics of chrysotile because calcite starts to decompose after the reaction of dehydroxylation of asbestos is fully accomplished and spinel is stable over the investigated range.

Isothermal kinetic XRPD data analysis

Reduced integrated intensities of chrysotile obtained by real-time XRPD were normalized to phase fractions (or normalized conversion factors α) and plotted as α vs. time curves. The plot generally has an increasing sigmoid shape in the case of a crystallization reaction and decreasing sigmoid shape in the case of a decomposition reaction.

The analysis of the kinetic curves was performed using the classical model for heterogeneous solid-state reactions described by the general expression of the Avrami–Erofe'ev equation (Bamford and Tipper 1980) $\alpha = 1 - \exp[(-kt)^n]$. The logarithmic transform of this equation is used to build a graph of $\ln[-\ln(1-\alpha)]$ vs. $\ln(t)$ in which isothermal experimental data are made linear in the so-called ln–ln plot where the reaction order (n) is calculated from the slope of the regression line whereas k, the rate coefficient, is calculated from the intercept. The experimental determination of the reaction order is a fundamental step for the interpretation of the reaction mechanism while the rate coefficient is utilized in the Arrhenius equation with T (in Kelvin) and R, the absolute gas constant: $k = A \cdot \exp[-E_a/RT]$. A plot of the $\ln(k)$ vs. $1/T$ yields the apparent activation energy (E_a) from the slope of the linear curve and the pre-exponential factor (A) from the line intercept (Bamford and Tipper 1980). The activation energy E_a represents the threshold enthalpy beyond which the transformation from reactants to products occurs. It is apparent because in real transformations it is usually constituted of a sum of several activation simultaneous processes. A is a statistic factor that represents the probability of an atom reaching the reaction-activated configuration. The logarithmic plots obtained by the isothermal kinetic curves of either the conventional or the synchrotron experiments are shown in Fig. 4. The relative Arrhenius plot is reported in Fig. 5. Table 1 reports the calculated n and k (rate constants) and the relative apparent activation energies and frequency factors. The relative standard deviations are reported in parentheses. The value of n denotes that the rate-limiting step of the reaction is a one-dimensional diffusion. Higher-dimensional diffusion or other mechanisms would be represented by higher values of n (Hulbert contribution in Bamford and Tipper 1980). A value of $n = 0.5$ implies an instantaneous nucleation (zero order) or a deceleratory rate of nucleation of the reaction product.

Discussion

The analysis of the TG curve (Fig. 2) and the results of the nonisothermal diffraction experiments (Fig. 3) indicate that the dehydroxylation reaction of clino-chrysotile

$$Mg_3Si_2O_5(OH)_4 \Rightarrow Mg_3Si_2O_7 + 2H_2O$$

in air starts at about 550 °C and is completed at 800 °C, corresponding with the nucleation and growth of forsterite according to the reaction

$$2Mg_3Si_2O_7 \Rightarrow 3Mg_2SiO_4 + SiO_2 \ .$$

Forsterite does not form directly from the chrysotile dehydroxylate, but an intermediate state exists. According to Martin (1977), the intermediate state is made up of semiamorphous material and preserves some of the original lattice order. MacKenzie and Meinhold (1994) define this early intermediate phase as dehydroxylate I with a number of distorted tetrahedral configurations.

We cannot exclude that the broad endothermic weight loss at about 700 °C is actually a two-step process caused by a multistage dehydroxylation reaction (Datta et al. 1986; MacKenzie and Meinhold 1994).

The sharp exothermic peak at about 800 °C is related to the latent heat of crystallization of forsterite as the diffraction peaks appear at that temperature. This result is in concert with Mackenzie (1972), but in contrast with MacKenzie and Meinhold (1994).

Because the decrease of the intensity of the peaks of chrysotile was monitored, the only reaction followed here was the dehydroxylation of chrysotile, i.e., the formation of the amorphous to diffraction precursor (or dehydroxylate-I according to MacKenzie and Meinhold

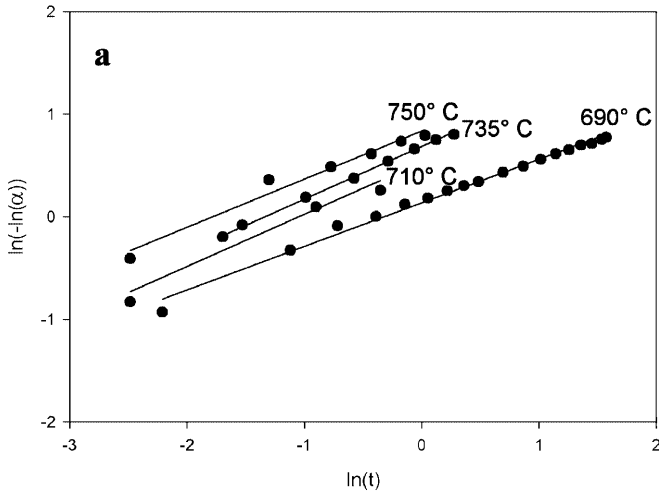

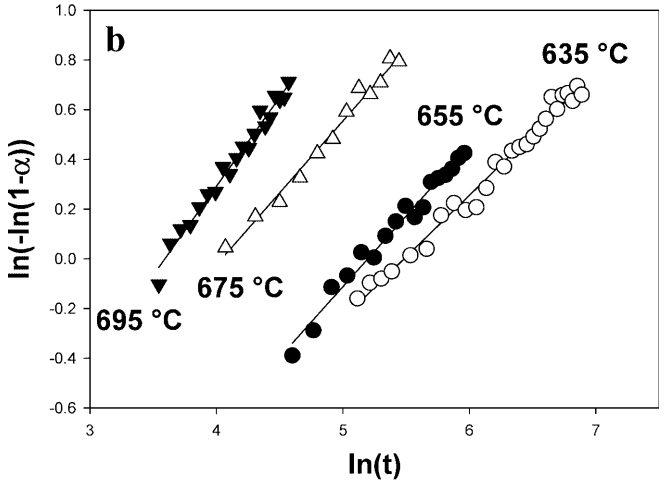

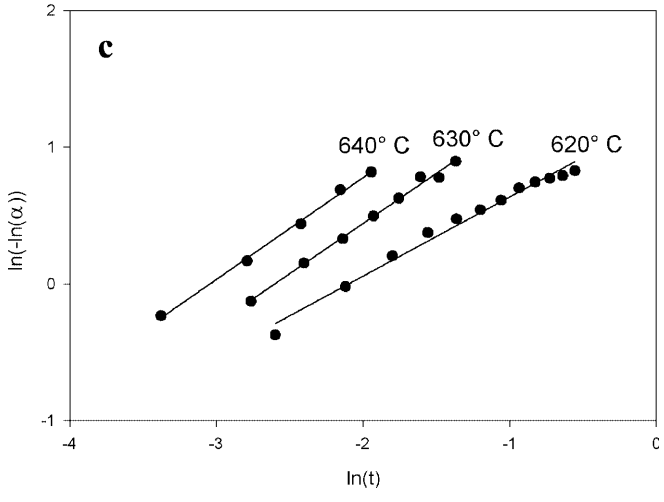

Fig. 4a–c ln–ln plot of the real-time conventional (**a**, **b**) and synchrotron (**c**) isothermal experimental runs collected at ESRF

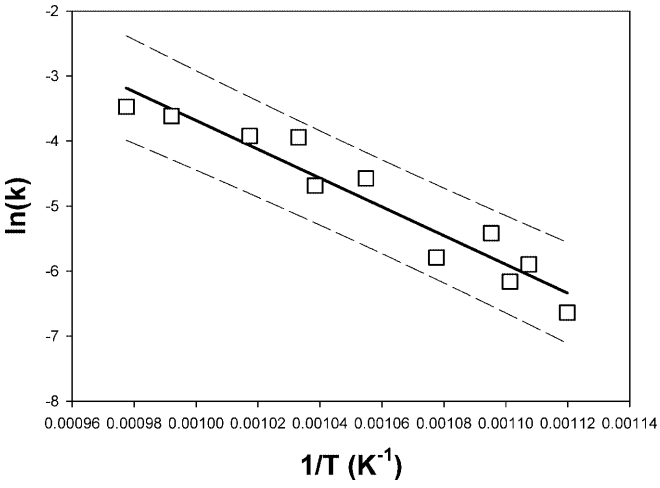

Fig. 5 Arrhenius plot for the calculation (the slope of the linear fit) of the apparent activation energy of the dehydroxylation reaction of chrysotile

1994) of forsterite and enstatite. The value of the order of the reaction mechanism indicates that the rate-limiting step of the reaction is a one-dimensional diffusion (Hulbert contribution in Bamford and Tipper 1980) with an instantaneous or deceleratory rate of nucleation. This is compatible with a one-dimensional diffusion of the water molecules formed in the interlayer region by direct condensation of two hydrogen atoms and one oxygen atom, a mechanism identical to that described for the decomposition of kaolinite (Bellotto et al. 1995). The calculated apparent activation energy (184 kJ mol^{-1}) is very similar to that of the ordered kaolinite (ca. 166–191 kJ mol^{-1}) whose rate-limiting step was the diffusion of protons or water molecules in the interlayer region. In both trioctahedral chrysotile (metachrysotile) and dioctahedral kaolinite dehydroxylate (metakaolinite), an amorphous precursor is the first product of the reaction sequence. For the chrysotile dehydroxylate, the same mechanism is observed, although diffusion is one-dimensional. To explain the reaction mechanism it is important to remind that chrysotile is a form of serpentine in which the lattice curves around itself to form tubular fibers which are circular or spiral in cross-section (Veblen and Wylie 1993). Thus, the possible one-dimensional escape paths for the water molecules are: radially (along the diameter of the fiber), perpendicular to the *b* axis (along the circumference of the cylindrical or spiral fibril forming the fibers), or along the *b* axis (along the fibril). The radial diffusion is unlikely because the water molecules should escape through the six-ring tetrahedral, a rate-limiting step postulated for the dehydroxylation reaction of muscovite (Mazzucato et al. 1999). In that case, the reaction temperature (760–860 °C) with the six-ring tetrahedral which open as a consequence of the thermal expansion and the calculated activation energy (255 kJ mol^{-1}) are higher than those observed here. The diffusion perpendicular to the *b* axis along the circumference of the fibrils is also unlikely because, especially in the cylindrical forms, the water molecules at some point would be forced to run in a circle with no way of escape. This is also the case of spiral forms, which are invariably distorted and interrupted.

Table 1 Calculated kinetic parameters for the dehydroxylation of chrysotile

	T (°C)	n	R^2	k	R^2
Synchrotron data	620	0.52(3)	0.984	0.00131(3)	0.984
	630	0.68(3)	0.988	0.00275(4)	0.980
	640	0.74(2)	0.995	0.0044(2)	0.996
		$\bar{n} = 0.65$			
Conventional data	635	0.49(3)	0.985	0.00211(6)	0.977
	655	0.57(4)	0.979	0.00306(5)	0.982
	675	0.58(3)	0.985	0.0103(6)	0.979
	695	0.72(4)	0.981	0.0194(6)	0.980
		$\bar{n} = 0.59$			
	690	0.41(1)	0.997	0.009(2)	0.913
	710	0.62(7)	0.937	0.019(5)	0.875
	735	0.63(2)	0.994	0.0269(2)	0.992
	750	0.66(7)	0.931	0.0310(6)	0.944
		$\bar{n} = 0.58$			
	E_a (kJ mol^{-1})	A	R^2		
	184(8)	1×10^8	0.930		

The preferred diffusion path is along *b*, i.e., along the fibril axis (Fig. 6). This model is confirmed by the direct TEM observations of Martin (1977), who found that long cavities opened within the (00*l*) planes in the fiber wall and extended along the fibers, indicating that a highly distorted tetrahedral layer is preserved. The tetrahedral layer must be very distorted, as MacKenzie and Meinhold (1994) reported the presence of a range of tetrahedral configurations in the phase designated dehydroxylate I. We cannot rule out that, as a consequence of the shrink of the O layer, the connected curved T layer releases the strain via O–Si–O bridge breaking, forming a number of isolated tetrahedra or two-membered tetrahedral clusters. We also cannot assess at which point the Si↔Mg cation migration takes place because the X-ray scattering cross-section of the two atoms is nearly identical and the peak resolution of our data is too poor. In conclusion, we cannot rule out that cation migration takes place before the collapse of chrysotile, as postulated by MacKenzie and Meinhold (1994).

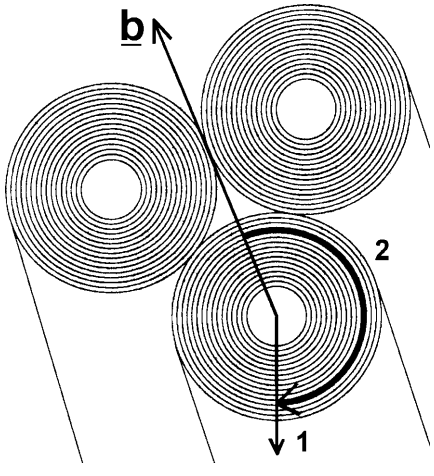

Fig. 6 One-dimensional possible diffusion paths of the water molecules in the reacting fibrils of chrysotile: radially along the diameter of the fiber *(1)*; along the circumference of the cylindrical or spiral fibril forming the fibers *(2)*; along the *b* axis

Our data show that the exothermic peak and forsterite growth are simultaneous, indicating that the exothermic peak at about 800 °C is actually the latent heat of formation of forsterite. This is in contrast with MacKenzie and Meinhold (1994), who found that the exotherm may be related to the collapse of the O layers with the separation of free silica, albeit it is very unlikely that heat is spontaneously released in that reaction.

The amorphous dehydroxylate of chrysotile is extremely unstable, readily clustering forsterite-rich and silica-rich regions. On the other hand, the amorphous (or pseudoamorphous) dehydroxylate of kaolinite (the so-called metakaolinite) is stable over a wider temperature interval, forming mullite above 950 °C (Gualtieri et al. 1995). The reason for such a difference could be the different nature of the two ions Mg^{2+} and Al^{3+}. If we consider their behavior in silicate melts, Mg^{2+} is a glass network modifier whereas Al^{3+} is a glass network former. Hence, crystallization is more favored in Mg^{2+}-rich glasses than in Al^{3+}-rich glasses. One of the consequences is that diffusion is easier for Al^{3+} than Mg^{2+} (diffusion activation energy is 125–210 kJ mol^{-1} for network modifiers and about 300 kJ mol^{-1} for network formers: Chakraborty 1995). We can safely rule out any dependence of the reactivity on the specimen morphology (i.e., it is not the fibrous habit which favors the high-temperature crystallization) because Brindley and Zussman (1957) reported that forsterite appears at about 600 °C in fibrous chrysotile or antigorite and at 650 °C in platy antigorite.

Literature data show that cytotoxicity of chrysotile towards human fibroblasts, red blood cells, and bovine alveolar macrophages was decreased by calcinations at low temperature (see references in Otero Areán et al. 2001). According to Otero Areán et al. (2001), this is due to a significant lowering of the capacity to trigger free radical generation, which is consistent with a dehydroxylation reaction. Hence, to reduce the hazard of chrysotile asbestos, an isothermal treatment at 800 °C for at least 4–5 h should result in a satisfactory yield of

transformation reaction to forsterite although a complete recrystallization to stable forsterite and enstatite is obtained by calcination at 1100 °C for 1 h (Gualtieri and Tartaglia 2000).

Conclusions

The kinetic of chrysotile dehydroxylation was followed by in situ XRPD in the range 620–750 °C. The calculated kinetic parameters indicate that the rate-limiting step of the reaction is one-dimensional diffusion with an instantaneous nucleation (zero order) or a deceleratory rate of nucleation, which implies a one-dimensional diffusion of the water molecules formed in the interlayer region by direct condensation of two hydroxyls. The calculated apparent activation energy of the process was 184 kJ mol^{-1}. By geometrical considerations, it is possible to demonstrate that the one-dimensional diffusion takes place along the fibril axis. The amorphous dehydroxylate of chrysotile is extremely unstable and forsterite is the first observed reaction product. The amorphous precursor is much less stable than the dehydroxylate of kaolinite (the so-called metakaolinite), which forms up to 950 °C. The difference is interpreted in terms of the different nature of the ion in the starting octahedral layer.

Acknowledgements This work is part of a COFIN project (04 Scienze della Terra, NR 17, 2000) supported by MURST. Dr Dapiaggi is kindly acknowledged for help during the data collection at the Dipartimento di Scienze della Terra, University of Milan.

References

Anselmi-Tamburini U, Campari G, Gigna P, Spinolo G (1993) An environmental chamber for powder diffractometers and for temperatures up to 1200 °C under various atmospheres and vacuum. Powder Diff 8: 210–213

Ball MC, Taylor HFW (1963) The dehydration of chrysotile in air and under hydrothermal conditions. Min Mag 33: 467–482

Bamford CH, Tipper CFH (1980) Comprehensive chemical kinetics. Elsevier, New York 22: 41–113

Bellotto M, Gualtieri AF, Artioli G, Clark SM (1995) Kinetic study of the kaolinite-mullite reaction sequence. Part I: kaolinite dehydroxylation. Phys Chem Miner 22: 207–214

Bish DL, Howard SA (1988) Quantitative phase analysis using the Rietveld-RIR method. J Appl Crystallogy 21: 86–91

Bowen NL, Tuttle OF (1949) The system MgO–SiO_2–H_2O. Bull Gèol Soc Am 60: 439–460

Brindley GW, Zussman J (1957) A structural study of the thermal transformation of serpentine minerals to forsterite. Am Mineral 42: 461–474

Brindley GW, Hayami R (1965) Mechanism of formation of forsterite and enstatite from serpentine. Min Mag 35: 189–195

Chakraborty S (1995) Diffusion in silicate melts. In: Structure, dynamics and properties of silicate melts. In: Stebbins JF, McMillan PF, Dingwell DB (eds) Reviews in mineralogy, vol. 32. Mineralogical Society of America, Washington, DC

Dapiaggi M, Artioli G, Petras L (2002) A newly developed high temperature chamber for in situ X-ray diffraction: setup and calibration procedures. Rigaku J 19: 35–41

Datta AK, Samantaray BK, Bhattacherjee S (1986) Thermal transformation of chrysotile asbestos. Bull Mat Sci 8: 497–503

Fubini B, Otero Areán C (1999) Chemical aspects of the toxicity of inhaled mineral dusts. Chem Soc Rev 28: 373–381

Gualtieri AF, Tartaglia A (2000) Thermal decomposition of asbestos and recycling in traditional ceramics. J Eur Ceram Soc 20: 1409–1418

Gualtieri A, Bellotto M, Artioli G, Clark SM (1995) Kinetic study of the kaolinite-mullite reaction sequence. Part II: mullite formation. Phys Chem Miner 22: 215–222

Gualtieri AF, Norby P, Artioli G, Hanson J (1977) Kinetics of formation of zeolite Na-A [LTA] from natural kaolinites. Phys Chem Minerals 24: 191–199

Hill RJ (1991) Expanded use of the Rietveld method in the studies of phase abundance in multiphase mixtures. Powder Diff 6: 74–77.

Guthrie GD (1992) Biological effects of inhaled minerals. Am Mineral 77: 225–243

Larson AC, Von Dreele RB (1994) GSAS Generalized structure analysis system. Laur 86–748, Los Alamos National Laboratory, Los Alamos, New Mexico

MacKenzie KJD, Meinhold RH (1994) Thermal reactions of chrysotile revisited: a ^{29}Si and ^{25}Mg MAS NMR study. Am Mineral 79: 43–50

MacKenzie RC (1972) Differential thermal analysis. Academic Press, London

Martin CJ (1977) The thermal decomposition of chrysotile. Miner Mag 35: 189–195

Mazzucato E, Artioli G, Gualtieri AF (1999) High-temperature dehydroxylation of muscovite-$2M_1$: a kinetic study by in situ XRPD. Phys Chem Miner 26: 375–381

Meneghini C, Artioli G, Balerna A, Gualtieri AF, Norby P, Mobilio S (2001) Multipurpose imaging-plate camera for in-situ powder XRD at the GILDA beamline. J Synch Rad 8: 1162–1166

Nelson B, Roy R (1954) New data on the composition and identification of chlorites. Clays and Clay Minerals 2: 335–348

Norby P (1997) Synchrotron powder diffraction using the imaging plates – crystal structure determination and Rietveld refinement. J Appl Crystallogr 30: 21–30

Otero Areán C, Barceló F, Fenoglio I, Fubini B, Llabrés FX, Xamena I, Tomatis M (2001) Free radical activity of natural and heat-treated amphibole asbestos. J Inorg Biochem 83: 211–216

Papirer E, Roland P (1981) Grinding of chrysotile in hydrocarbons, alcohol and water. Clays Clay Miner 29: 161–170

Rietveld HM (1969) A profile refinement method for nuclear and magnetic structures. J Appl Crystallogr 2: 65–71

Suquet H (1989) Effects of dry grinding and leaching on the crystal structure of chrysotile. Clays Clay Miner 37: 439–445

Swenson CA (1983) Recommended values for the thermal expansivity of silicon from 0 to 1000 K. J Phys Chem 12 (2): 179–181

Veblen DR, Wylie AG (1993) Mineralogy of amphiboles and 1:1 layer silicates. In: Guthrie GD Jr, Mossman BT (eds) Health effects of mineral dusts. Mineralogical Society of America, vol 28. Washington, DC, pp 139–181

Wicks FJ, O'Hanley DS (1988) Serpentine minerals: structures and petrology. In: Bailey SW (ed) Hydrous phillosilicates. Mineralogical Society of America, vol. 19, Washington, DC, pp 91–188